Electron-Impact Ionization Cross Sections for Polyatomic Molecules, Radicals, and Ions

Yong-Ki Kim and Karl K. Irikura

National Institute of Standards and Technology, Gaithersburg, Maryland 20899 U.S.A.

Abstract. The binary-encounter-Bethe (BEB) model for calculating electron-impact ionization cross sections for molecules is described with emphasis on polyatomic molecules and their radicals and ions. The BEB model provides an analytic formula for the cross section. The formula is for each molecular orbital, and requires only three numbers from the initial state of the target molecule: the electron occupation number, the orbital binding energy, and the orbital kinetic energy. The sum of the orbital cross sections provides the molecular cross section. The BEB model produces reliable ionization cross sections from the threshold to several keV in incident electron energy for neutral molecules and ions. The BEB cross sections for some fluorine-containing radicals are almost a factor of two larger than available experimental values. Molecular constants are included to generate BEB cross sections for H_2, C_2F_6, H_2^+, CH_3, CF_x, BF_x, BCl_x for x=1-3, and several unsaturted molecules relevant to hydrocarbon combustion.

1. INTRODUCTION

Electron-impact ionization cross sections of atoms and molecules are important not only for the development of basic collision theory, but also in a wide range of practical applications. For instance, the modeling of semiconductor manufacturing by plasma processing requires ionization cross sections of fluorocarbons used as the feed gas, their ions and fragments. Hydrocarbon molecules, such as methane, are found in the vicinity of divertors in a fusion device, making it necessary to include ionization of such molecules to model low-temperature plasmas in tokamaks. Ionization cross sections near the ionization threshold are also used in modeling combustion of flammable gases. In this article, we describe a simple, effective theory—the binary-encounter-Bethe (BEB) model—to calculate electron-impact ionization cross sections for large and small molecules, including their fragments and ions.

The BEB model combines a modified form of the Mott cross section and the dipole-interaction term of the plane-wave Born approximation. The original Mott cross section [1] is for the collision of two free electrons. This formula must be modified to include the binding energy B, so that the cross section does not diverge, as the original Mott cross section does, for the ejection of an electron with a very low kinetic energy W. Using the plane-wave Born approximation, Bethe has shown [2] that the leading term of the Born cross section at high incident electron energy T represents the

CP543, *Atomic and Molecular Data and Their Applications,* edited by K. A. Berrington and K. L. Bell
2000 American Institute of Physics 1-56396-971-8

dipole interaction between the incident and the target electrons. The dipole interaction is characteristic of a bound electron, and the Mott cross section lacks this feature.

Since the Mott cross section is derived using a Coulomb function for the incident electron while the Born approximation uses a plane wave, these two theories cannot be simply added. In the past, many attempts were made to combine the Mott and Born cross sections mostly by introducing empirical parameters. Kim and Rudd [3] have succeeded in combining the two types of cross sections without introducing any adjustable or empirical parameters. They required that both the combined ionization cross section and the matching stopping cross section (integral of energy transfer times ionization cross section) satisfy the correct asymptotic (high T) forms derived by Bethe [2,4].

Kim and Rudd [3] combined differential ionization cross sections, which used continuum dipole oscillator strength $f(E)$ with energy transfer E. In principle $f(E)$ can be deduced from photoionization cross sections. What is required in their theory, however, is $f(E)$ for each molecular orbital, not just the total photoionization cross section. Often details of $f(E)$ for each orbital are available only for simple molecules such as H_2. When the weighted integral of $f(E)$ shown in Eq. (2) is known, we get a simple expression for the integrated cross section—i.e., integrated over the secondary electron energies W—which we refer to as the BEQ cross section:

$$\sigma_{\mathrm{BEQ}}=\frac{S}{t+u+1}\left[\frac{Q}{2}\ln t\left(1-\frac{1}{t^2}\right)+(2-Q)\left(1-\frac{1}{t}-\frac{\ln t}{1+t}\right)\right], \tag{1}$$

$$Q=\frac{2BM_i^2}{NR}, \quad \text{with} \quad M_i^2=\frac{R}{B}\int_B^\infty \frac{B}{E}f(E)\mathrm{d}E, \tag{2}$$

where, $S=4\pi a_0^2 N(R/B)^2$, a_0 is the Bohr radius, R is the Rydberg energy, N is the electron occupation number, $t = T/B$, $u = U/B$, and U is the orbital kinetic energy.

When $f(E)$ is unknown, we can approximate $Q = 1$, and obtain the BEB equation:

$$\sigma_{\mathrm{BEB}}=\frac{S}{t+u+1}\left[\frac{\ln t}{2}\left(1-\frac{1}{t^2}\right)+1-\frac{1}{t}-\frac{\ln t}{1+t}\right]. \tag{3}$$

The first logarithmic term in Eq. (3) represents the dipole interaction from the Born approximation, $1-1/t$ originates from the direct and exchange collision terms in the Mott cross section, and the last logarithmic term stands for the interference between the direct and exchange collision terms. Unlike conventional collision theories, the BEB model does not explicitly use the final state of the target. The only quantity linked to the final state of the ion is the binding energy B. As in the case of photoionization, vertical ionization energy should be used for B.

The BEB cross section is sensitive to the ionization energies for outer valence orbitals, while inner shell binding energies need not be very accurate. For the examples shown in this article, the binding energies for inner-shell orbitals were approximated by the orbital energies from restricted Hartree-Fock or equivalent

molecular wave functions, while experimental values or results from correlated wave functions were used for outer valence orbitals.

In Sec. 2 we compare BEB cross sections to experimental data for neutral molecules, molecular ions, and radicals to demonstrate the utility of the BEB model. Computational details for the molecular wave functions are described in Sec. 3, our conclusion is presented in Sec. 4, and molecular constants to generate BEQ/BEB cross sections for a number of molecules are listed in Table 1.

2. COMPARISONS TO EXPERIMENTS

In this section, we present comparisons of the BEB cross sections to available experimental data. In general the total ionization cross section is measured by two different methods: (a) measure the total ion current, or (b) measure partial cross sections for fragment ions and then the partial cross sections are summed to deduce the total ionization cross section. Method (a) produces the gross total ionization cross section, in which multiply charged ions are weighted by their net charge n:

$$\sigma_{gross} = \Sigma\, n\sigma_{n+},$$

where σ_{n+} is the cross section for producing an n-times charged ion. On the other hand, method (b) leads to the counting total ionization cross section:

$$\sigma_{count} = \Sigma\, \sigma_{n+}.$$

A straightforward sum of BEB orbital cross sections corresponds to the counting total ionization cross section. To emulate the gross ionization cross section, we must multiply BEB orbital cross sections for some inner shells by appropriate net charge n. For instance, a hole created by ionizing an inner orbital whose binding energy is larger than the energy needed to produce a doubly charged ion will decay by the Auger process. A hole in a very deep inner shell may even lead to the production of triply and quadruply charged ions. Such a highly charged molecular ion, however, is unstable and eventually breaks up into singly charged fragments. Besides, the cross sections for such deep inner-shell orbitals are insignificant compared to the large ionization cross sections of valence orbitals. Hence, we found that it is sufficient in most cases to account only for the production of doubly charged ions for comparison to experimental gross ionization cross sections. Whether a doubly charged molecular ion breaks up into two singly charged fragments or not, we found that doubling the cross sections for orbitals, whose binding energies are in the range of about 30 to 200 eV and exceed the double ionization energy, led to reliable gross ionization cross sections.

The gross ionization cross section deduced from the method (b) by multiplying partial cross sections by n before summing them does not necessarily agree with the gross ionization cross section from the method (a) because some σ_{n+} are too small to be measured.

2.1. Comparisons for Neutral Molecules

In Fig. 1, we compare the BEQ cross section for H_2 to other theories and available

experimental data. The triangles marked DM in Fig. 1 represent the semiempirical theory by Deutsch et al. [5], which is based on a modified form of Gryzinski's classical theory [6] and commonly referred to as the DM formalism.

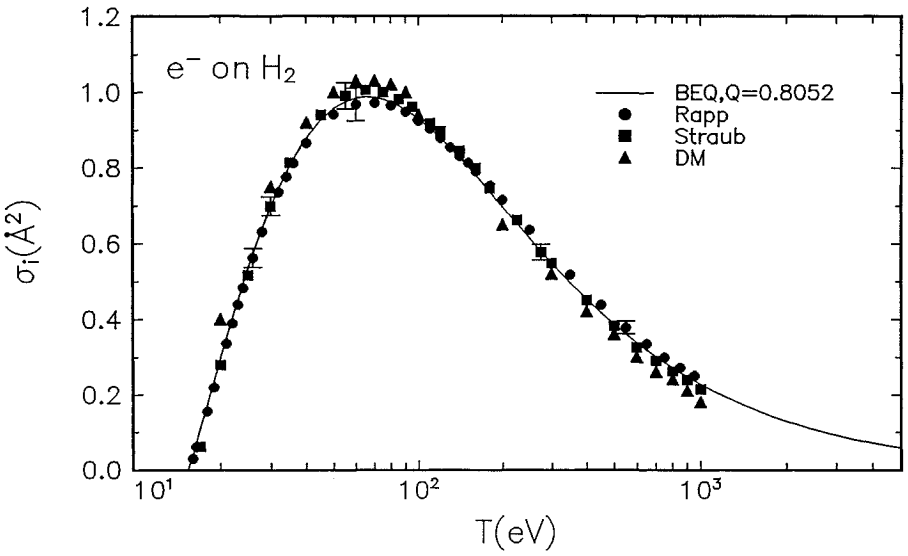

FIGURE 1. Electron-impact total ionization cross section of H_2. Solid curve, the BEQ cross section, Eq. (1); circles, experimental data by Rapp and Englander-Golden [7]; squares, data by Straub et al. [8]; triangles, semiempirical theory by Deutsch et al. [5].

The BEQ cross section in Fig. 1 is in excellent agreement with the benchmark experiments by Rapp and Englander-Golden [7] (with total uncertainties of ±4%) and by Straub et al. [8] (with total uncertainties of ±3.5%). *We recommend use of the BEQ cross section as the normalization standard for the total ionization cross section of H_2.* The recommended cross section should be reliable to ±5%. The molecular constants for H_2 along with those for other molecules are listed in Table 1.

Large molecules with many bound electrons tend to have many valence orbitals with low ionization energies. For such molecules, the orbital binding energies B are sensitive to the quality of the molecular wave function, though the orbital kinetic energy $U=\langle \boldsymbol{p}^2/2m \rangle$ with the usual notation are not because it is an expectation value of a one-electron operator. As an example, we compare in Fig. 2 available experimental and semiempirical cross sections for C_2F_6 to the BEB cross sections calculated from a restricted Hartree-Fock (RHF) wave function and from correlated, complete-active-space (CAS) wave functions.

The solid curve in Fig. 2 includes theoretical estimates for double ionization. The correlated wave functions lead to lower ionization energies for valence orbitals, which in turn produce higher orbital cross sections. The effect of electron correlation can be as much as 20% [9] for large molecules. The semiempirical DM formalism tends to produce low cross sections at high T because the classical theory, upon which the DM

cross sections are based, lacks the dipole interaction which is dominant at high T. The molecular constants for the BEB cross section of C_2F_6 are listed in Table 1.

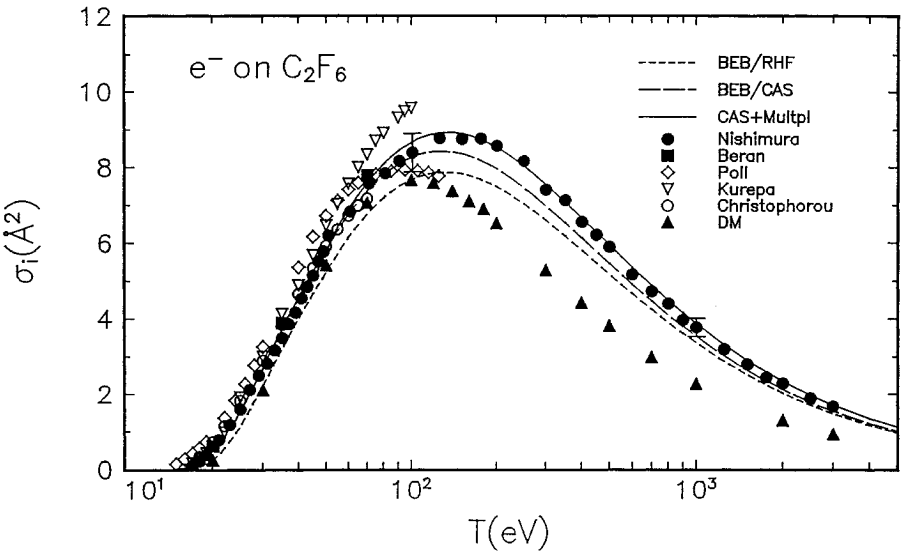

FIGURE 2. Electron-impact total ionization cross section of C_2F_6. Solid curve, BEB σ_{gross} from correlated wave functions; long-dashed curve, BEB σ_{count} from correlated wave functions; short-dashed curve, BEB σ_{count} from an uncorrelated wave function; filled circles, experimental σ_{gross} by Nishimura et al. [9]; filled squares, experimental σ_{gross} by Beran and Kevan [10]; open diamonds, experimental σ_{count} by Poll and Meichsner [11]; open triangles, σ_{gross} by Kurepa [12]; open circles, σ_{gross} adopted by Christophorou and Olthoff [13]; filled triangle, semiempirical DM formalism [5].

Hwang et al. [14] reported that known experimental cross sections for valence orbitals with $n \geq 3$ and primarily atomic character--as indicated by a Mulliken population of 85% or higher--are reproduced well when u in the denominators of Eqs. (1) and (3) is reduced. Currently, *we recommend replacing* u+1 *by* $(u+1)/n$ *for* $n \geq 3$.

For molecules containing very heavy elements, such as WF_6, orbital data from relativistic wave functions are desirable. Although computer codes to calculate relativistic wave functions for atoms are readily available, relativistic wave functions for polyatomic molecules are scarce and time consuming to calculate. Instead, one can use molecular orbital data obtained from an effective core potential as is commonly done. The use of an effective core potential has another advantage: for atomic orbitals with high principal quantum numbers n, the orbital kinetic energies remain low because inner radial function nodes have been eliminated in such a calculation [15].

In Fig. 3, we compare the BEB σ_{count} calculated using a relativistic effective core potential for WF_6 with recent experimental and semiempirical cross sections. This is one area where we need more experimental data to assess the validity of the BEB model for molecules containing heavy atoms.

Heavy atoms have many inner-shell orbitals with $n \geq 3$. Except for the outermost

valence orbitals, Kim et al. [16] found an alternative to dividing u+1 by n, i.e., take a simple average of Eq. (3) and the same equation with the denominator t+u+1 replaced by t,

$$\sigma_{BEBav} = \tfrac{1}{2}[1 + (t+u+1)/t] \times \text{Eq. (3)}, \qquad (4)$$

for inner orbitals with $n \geq 3$.

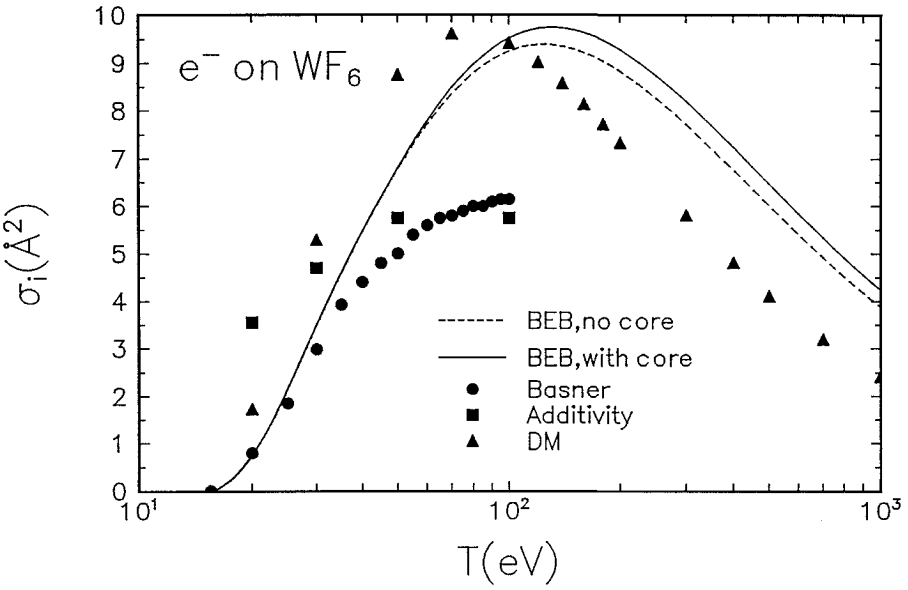

FIGURE 3. Electron-impact ionization cross section of WF_6. Solid curve, BEB σ_{count} calculated from an effective core potential plus core cross sections calculated from atomic core wave functions for W; dashed curve, same as the solid curve minus the contribution from the W core; circles, experimental data by Basner et al. [17]; squares, semiempirical additivity-rule cross section by Deutsch et al. [18]; triangles, semiempirical DM formalism by Deutsch et al. [5].

2.2 Comparison for Molecular Ions

Unlike atomic ions, molecular ions with a net charge of 2 or higher are unstable, and hence we need to adapt the BEB model only to singly-charged molecular ions. Kim and Rudd [3] noted that u+1 had to be reduced for atomic ions because the correlation between the incident electron and a target ion is different than a neutral target. For singly-charged ions, *we recommend replacing* u+1 *in Eqs.* (1) *and* (3) *by* (u+1)/2. For molecular ions containing heavy atoms, we do not have any experimental data to compare. Judging from our limited experience with heavy atomic ions, we suggest using σ_{BEBav} defined by Eq. (4) for the core orbitals ($n \geq 3$) of heavy atoms in molecules.

We compare in Fig. 4 the experimental data by Peart and Dolder [19] for H_2^+ to the BEQ and BEB cross sections using (u+1)/2. Comparisons of the BEB cross sections to experimental data for N_2^+ and CD^+ also show good agreement [20]. Since a simple

dissociation of a molecular ion without ionizing any electron still produces an ion, the determination of experimental data for the ionization of a molecular ion is much more difficult than that for the ionization of a neutral molecule.

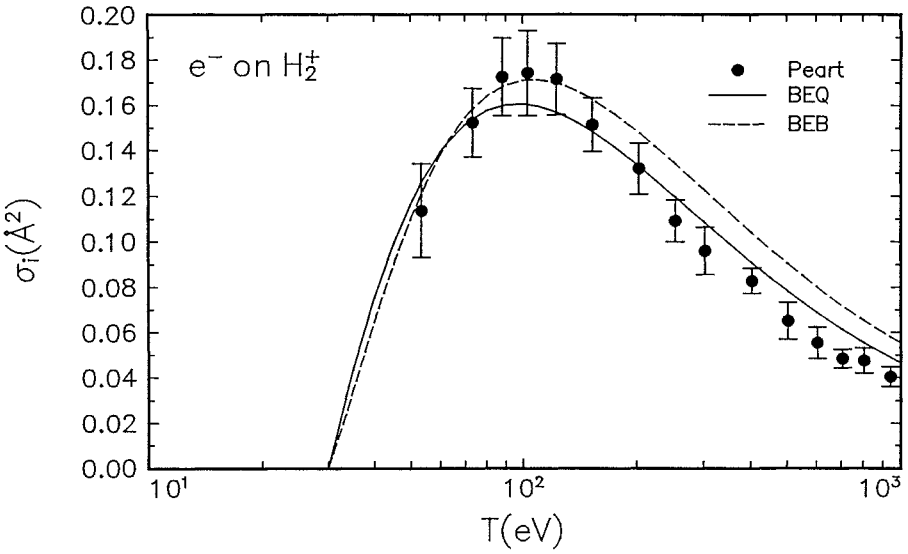

FIGURE 4. Electron-impact total ionization cross section of H_2^+ [20]. Solid curve, BEQ cross section with $(u+1)/2$; dashed curve, BEB cross section with $(u+1)/2$; circles, experimental data by Peart and Dolder [19].

2.3 Comparisons for Radicals

The BEB model treats a neutral radical or fragment the same as a neutral, stable molecule, i.e., Eqs. (1) or (3) are used. Radicals often have open-shell configurations, and one must be careful in generating molecular data for such a system. Also, experimental data on radicals are rare and often unreliable because of the difficulty in making enough target molecules.

In Fig. 5, we compare the BEB cross section for CD_3 to available experimental and semiempirical data. Although experiments used CD_3 [21,22], the BEB cross section is for CH_3 because the theory does not distinguish isotopes. We found that the BEB cross sections on other hydrocarbon radicals are in excellent agreement with available experiments [14,23].

In contrast, we find nearly a factor of two disagreement between the BEB cross sections and experimental data on fluorine containing molecules, such as CF_x, and NF_x. We compare in Fig. 6 the BEB cross section and experimental data by Becker [24] and by Tarnovsky et al. [25] for CF_3. The experimental data in Figs. 5 and 6 were taken by the same group using the same apparatus. At present, we do not understand the large discrepancy in Fig. 6, except for the possibility that the resulting ions of CF_3

dissociate in such a way as to escape detection by the apparatus used. The dashed curve in Fig. 6 is the BEB cross section which includes only those orbitals with $B <$ 19 eV. The threshold for dissociative ionization of CF_3 is approximately 19 eV.

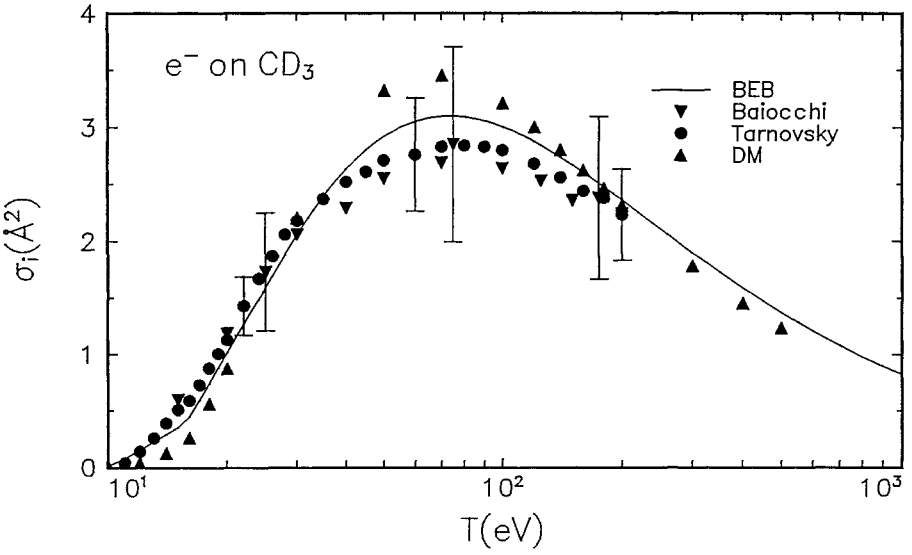

FIGURE 5. Electron-impact total ionization cross section of CD_3. Solid curve, BEB cross section for CH_3; inverted triangles, experimental data by Biocchi et al. [21]; circles, experimental data by Tarnovsky et al. [22]; upright triangles, semiempirical DM formalism by Deutsch et al. [5].

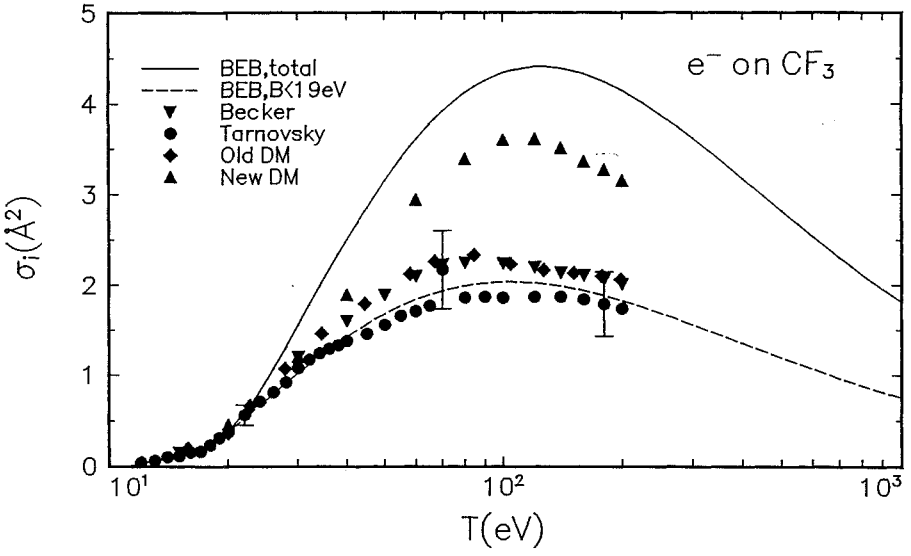

FIGURE 6. Electron-impact total ionization of CF_3. Solid curve, the BEB cross section; dashed curve,

the BEB cross section for orbitals with $B < 19$ eV; inverted triangles, experimental data by Becker [24]; circles, experimental data by Tarnovsky et al. [25], diamonds, semiempirical additivity rule by Deutsch et al. [18]; upright triangles, semiempirical DM formalism [5].

3. DETAILS OF MOLECULAR CALCULATIONS

Different ab initio methods yield different values for molecular properties. In particular, orbital binding energies (B) depend upon the theoretical method employed. Thus, the details of the molecular orbital calculations affect the final predictions for ionization cross sections. In general, more thorough calculations include more electron correlation, which reduces values of B and increases the predicted cross sections.

Binding and kinetic energies are insensitive to molecular geometry. We generally use geometries that are calculated using the nonlocal B3LYP density functional (a parameterized exchange functional [26] and a fitted correlation functional [27]) in combination with the 6-31G(d) basis of atom-centered Gaussian functions [28].

Since the final cross sections are especially sensitive to the value of the lowest binding energy, we use either experimental vertical ionization energies, typically from photoelectron spectra, or theoretical values computed using the CCSD(T) method (coupled-cluster theory including the single- and double-excitation operators [29] and a perturbative estimate of connected triples [30]) combined with the polarized, valence-triple-zeta basis designated cc-pVTZ [31,32]. We expect these CCSD(T) binding energies to be reliable to about 0.1 eV or better.

Binding energies for the other valence orbitals are computed either using the outer-valence Green's function (OVGF) method [33,34] or the uncorrelated Hartree-Fock method (HF), both with the diffuse 6-311+G(d,p) basis as defined in the Gaussian 98 computer code [35]. Orbital kinetic energies are computed using HF theory and the 6-311G(d,p) basis as defined in the GAMESS program [36].

Thresholds for double ionization should be the adiabatic values instead of the vertical values. Analogously to the vertical single ionization energies, double ionization thresholds were computed at the CCSD(T)/cc-pVTZ level using B3LYP/6-31G(d) geometries. In several cases, however, the doubly-charged ion is unbound, and we adopt the vertical double ionization energy instead. This is typically computed at the correlated OVGF/6-311G(d,p) level.

All single-reference, open-shell calculations are done using a spin-unrestricted (UHF) reference, which involves spatially distinct α and β orbitals (one electron per orbital). This can lead to very long tables of molecular orbital data. The α/β orbital pairs may usually be averaged together with negligible effect on the computed cross sections. For conciseness, we have done this in preparing Table 1, except where averaging caused more than about 1% change in the final cross sections.

4. CONCLUSIONS

We have presented comparisons of the BEB cross sections to available experimental and other theoretical data on small and large neutral molecules, molecular ions, and

Table 1. Molecular orbital constants to generate the BEQ/BEB cross sections [see Eqs. (1) and (3)]. Q=1 unless noted in the table. Only orbital cross sections marked Dbl=Y are doubled to account for double ionization. Orbitals that are essentially atomic with $n \geq 3$ are indicated in the "AO" column.

Molecule	Orbital	B(eV)	U(eV)	N	Q	Dbl	AO	Remarks
H_2^+	1σ	30.00	16.40	1	0.5275			
H_2	1σ	15.43	15.98	2	0.8052			Adiabatic B
CD_3/CH_3	$1a_1'$	305.45	436.19	2		Y		UHF (averaged)
	$2a_1'$	22.76	34.12	2				B from OVGF
	$1e'$	15.09	26.31	4				B from OVGF
	$1a_2''$	9.84	29.81	1				Vertical B from exper.
C_2F_6	$1e_g$	718.05	1013.49	4				CASSCF
	$1e_u$	718.05	1013.50	4				
	$1a_{2u}$	718.05	1013.51	2				
	$1a_{1g}$	718.05	1013.53	2				
	$2a_{1g}$	314.56	436.28	2				
	$2a_{2u}$	314.55	436.53	2				
	$3a_{1g}$	48.90	88.82	2		Y		
	$3a_{2u}$	48.16	94.16	2		Y		
	$2e_u$	46.05	103.39	4		Y		
	$2e_g$	45.60	107.04	4		Y		
	$4a_{1g}$	29.74	69.84	2				
	$4a_{2u}$	26.56	83.75	2				
	$5a_{1g}$	24.98	65.27	2				
	$3e_u$	24.12	74.26	4				
	$3e_g$	23.17	78.30	4				
	$5a_{2u}$	20.69	84.03	2				
	$4e_g$	20.86	82.12	4				
	$4e_u$	19.82	87.85	4				
	$5e_u$	18.42	88.57	4				
	$5e_g$	16.38	95.04	4				
	$6a_{1u}$	16.58	95.50	2				
	$6a_{2g}$	17.41	93.54	2				
	$7a_{1g}$	14.5	79.89	2				Vertical B from exper.
BF	1σ	717.85	1013.53	2		Y		
	2σ	210.08	297.18	2		Y		
	3σ	46.25	104.14	2		Y		
	4σ	21.71	84.12	2				B from OVGF
	1π	18.78	80.94	4				B from OVGF
	5σ	11.13	27.52	2				B from CCSD(T)
BF_2	$1b_2$	716.80	1013.50	2		Y		UHF (averaged)
	$1a_1$	716.80	1013.51	2		Y		
	$2a_1$	211.09	296.86	2		Y		

	$3a_1$	45.41	101.31	2	Y		
	$2b_2$	44.65	105.56	2	Y		
	$4a_1$	21.49	80.69	2			B from OVGF
	$3b_2$	20.00	81.97	2			B from OVGF
	$1b_1$	18.62	75.74	2			B from OVGF
	$5a_1$	18.59	77.06	2			B from OVGF
	$1a_2$	17.11	85.72	2			B from OVGF
	$4b_2$	16.84	89.92	2			B from OVGF
	$6a_1$	10.28	40.51	1			B from CCSD(T)
BF_3	1e'	716.93	1013.47	4	Y		
	$1a_1$'	716.93	1013.48	2	Y		
	$2a_1$'	212.33	296.73	2	Y		
	$3a_1$'	46.01	98.98	2	Y		
	2e'	44.86	105.18	4	Y		
	$4a_1$'	21.77	82.01	2			B from OVGF
	3e'	20.48	78.08	4			B from OVGF
	$1a_2$"	19.20	72.16	2			B from OVGF
	4e'	17.05	87.51	4			B from CCSD(T)
	1e"	16.77	85.72	4			B from CCSD(T)
	$1a_2$'	15.99	92.90	2			B from CCSD(T)
BCl	1σ	2853.82	3731.10	2	Y		
	2σ	288.57	593.27	2	Y		
	3σ	219.65	561.36	2	Y		
	1π	219.60	561.81	4	Y		
	4σ	210.31	297.39	2	Y		
	5σ	31.42	77.17	2	Y	3s	
	6σ	17.09	56.50	2			B from OVGF
	2π	13.49	57.24	4		3p	B from OVGF
	7σ	10.20	31.95	2			B from CCSD(T)
BCl_2	$1b_2$	2853.45	3731.10	2	Y		UHF (averaged)
	$1a_1$	2853.45	3731.10	2	Y		
	$2b_2$	288.19	593.26	2	Y		
	$2a_1$	288.19	593.27	2	Y		
	$3b_2$	219.30	561.36	2	Y		
	$3a_1$	219.30	561.36	2	Y		
	$1b_1$	219.22	561.81	2	Y		
	$1a_2$	219.22	561.82	2	Y		
	$4b_2$	219.20	561.86	2	Y		
	$4a_1$	219.20	561.86	2	Y		
	$5a_1$	210.64	297.01	2	Y		
	$6a_1$	31.52	73.63	2	Y		
	$5b_2$	30.52	80.44	2	Y	3s	
	$7a_1$	17.29	57.81	2			B from OVGF

	$6b_2$	15.02	59.26	2			B from OVGF
	$8a_1$	13.59	51.77	2			B from OVGF
	$2b_1$	13.59	53.19	2		3p	B from OVGF
	$2a_2$	12.31	61.36	2		3p	B from OVGF
	$7b_2$	12.06	64.28	2		3p	B from OVGF
	$9a_1$	8.75	45.19	1			B from CCSD(T)
BCl_3	1e'	2853.46	3731.1	4	Y		
	$1a_1$'	2853.46	3731.1	2	Y		
	2e'	288.2	593.24	4	Y		
	$2a_1$'	288.2	593.26	2	Y		
	3e'	219.3	561.2	4	Y		
	$3a_1$'	219.3	561.2	2	Y		
	1e"	219.24	561.82	4	Y		
	$1a_2$"	219.24	561.81	2	Y		
	4e'	219.23	561.98	4	Y		
	$1a_2$'	219.23	561.98	2	Y		
	$4a_1$'	211.86	297	2	Y		
	$5a_1$'	32.19	70.01	2	Y		
	5e'	30.56	80.15	4	Y		
	$6a_1$'	17.78	60.57	2			B from OVGF
	6e'	15.42	56.01	4			B from OVGF
	$2a_2$"	14.09	49.92	2			B from OVGF
	7e'	12.54	62.79	4		3p	B from CCSD(T)
	2e"	12.34	61.43	4		3p	B from CCSD(T)
	$2a_2$'	11.68	67.06	2		3p	B from CCSD(T)
C_2H_3	1a'	306.18	435.63	2	Y		UHF (averaged)
(vinyl)	2a'	305.51	436.63	2	Y		
	3a'	28.13	42.5	2			
	4a'	19.23	33.39	2			B from OVGF
	5a'	15.84	30.43	2			B from OVGF
	6a'	14.9	29.73	2			B from OVGF
	1a"	10.61	27.82	2			B from OVGF
	7a'	9.54	33.52	1			B from CCSD(T)
C_3H_3	$1a_1$	306.36	435.55	2	Y		UHF (averaged)
(propargyl)	$2a_1$	305.99	436.01	2	Y		
	$3a_1$	305.57	436.54	2	Y		
	$4a_1$	28.98	45.42	2	Y		
	$5a_1$	22.68	42.88	2			B from OVGF
	$6a_1$	18.11	33.63	2			B from OVGF
	$7a_1$	16.12	36.64	2			B from OVGF
	$1b_2$	15.58	26.27	2			B from OVGF
	$1b_1$	11.52	28.38	2			B from OVGF
	$2b_2$	10.38	29.8	2			B from OVGF
	$2b_1$	8.55	32.44	1			B from CCSD(T)

C_3H_4	$1a_1$	306.53	436.08	2	Y	
(allene)	$1b_2$	305.88	436.06	2	Y	
	$2a_1$	305.88	436.13	2	Y	
	$3a_1$	29.27	43.81	2	Y	
	$2b_2$	26.11	41.25	2	Y	
	$4a_1$	17.64	35.54	2		B from OVGF
	$3b_2$	15.47	37.09	2		B from OVGF
	1e	15.1	26.1	4		B from OVGF
	2e	10.22	28.21	4		B from CCSD(T)
C_3H_5	$1a_1$	305.82	435.71	2	Y	UHF (averaged)
(allyl)	$1b_2$	305.50	436.13	2	Y	
	$2a_1$	305.37	436.52	2	Y	
	$3a_1$	29.06	40.11	2	Y	
	$2b_2$	22.22	38.53	2		B from OVGF
	$4a_1$	18.90	32.55	2		B from OVGF
	$5a_1$	16.38	26.98	2		B from OVGF
	$3b_2$	15.04	32.24	2		B from OVGF
	$4b_2$	13.65	32.38	2		B from OVGF
	$6a_1$	12.96	30.58	2		B from OVGF
	$1b_1$	10.94	26.63	2		B from OVGF
	$1a_2$	8.02	31.57	1		B from CCSD(T)
C_3H_4	$1a_1$	306.24	436.09	2	Y	
(propyne)	$2a_1$	305.82	435.95	2	Y	
	$3a_1$	305.38	436.14	2	Y	
	$4a_1$	28.80	42.70	2	Y	
	$5a_1$	26.10	42.28	2		
	$6a_1$	17.80	33.68	2		B from OVGF
	$7a_1$	15.39	37.09	2		B from OVGF
	1e	15.02	25.75	4		B from OVGF
	2e	10.48	29.49	4		B from CCSD(T)
C_3H_6	1a'	305.79	436.13	2	Y	
(propene)	2a'	305.45	436.14	2	Y	
	3a'	305.34	436.15	2	Y	
	4a'	28.97	38.93	2	Y	
	5a'	22.58	37.25	2		B from OVGF
	6a'	18.68	32.93	2		B from OVGF
	7a'	15.90	27.01	2		B from OVGF
	8a'	14.57	32.04	2		B from OVGF
	1a"	14.50	25.17	2		B from OVGF
	9a'	13.29	31.14	2		B from OVGF
	10a'	12.36	31.12	2		B from OVGF
	2a"	9.95	27.25	2		B from CCSD(T)

C_4H_2	$1\sigma_g$	306.70	435.59	2	Y	
(diacet-	$1\sigma_u$	306.67	435.92	2	Y	
ylene)	$2\sigma_g$	306.48	436.23	2	Y	
	$2\sigma_u$	306.47	436.28	2	Y	
	$3\sigma_g$	29.78	47.66	2	Y	
	$3\sigma_u$	27.84	49.54	2	Y	
	$4\sigma_g$	20.55	43.58	2		B from OVGF
	$4\sigma_u$	17.97	33.91	2		B from OVGF
	$5\sigma_g$	17.24	36.45	2		B from OVGF
	$1\pi_u$	12.51	27.78	4		B from OVGF
	$1\pi_g$	10.19	30.47	4		B from CCSD(T)
C_4H_4	1a'	306.59	436.06	2	Y	
(vinyl-	2a'	306.20	436.16	2	Y	
acetylene)	3a'	305.98	435.86	2	Y	
	4a'	305.73	436.23	2	Y	
	5a'	29.76	42.66	2	Y	
	6a'	27.41	46.97	2	Y	
	7a'	23.01	38.87	2		
	8a'	17.79	32.83	2		B from OVGF
	9a'	16.54	30.84	2		B from OVGF
	10a'	15.32	35.72	2		B from OVGF
	11a'	13.53	31.07	2		B from OVGF
	1a"	11.99	26.34	2		B from OVGF
	12a'	10.47	29.97	2		B from OVGF
	2a"	9.63	29.11	2		B from CCSD(T)
C_4H_6	$1a_g$	305.97	435.95	2	Y	
(trans-	$1b_u$	305.95	436.22	2	Y	
butadiene)	$2a_g$	305.69	436.17	2	Y	
	$2b_u$	305.69	436.18	2	Y	
	$3a_g$	29.76	40.25	2	Y	
	$3b_u$	27.27	41.50	2	Y	
	$4a_g$	22.56	37.60	2		
	$4b_u$	18.51	30.46	2		B from OVGF
	$5b_u$	15.85	31.33	2		B from OVGF
	$5a_g$	15.58	28.72	2		B from OVGF
	$6a_g$	13.72	37.67	2		B from OVGF
	$6b_u$	13.62	29.62	2		B from OVGF
	$7a_g$	12.31	31.34	2		B from OVGF
	$1a_u$	11.54	24.83	2		B from OVGF
	$1b_g$	9.14	27.78	2		B from CCSD(T)
C_4H_8	1a	305.71	436.11	2	Y	
(1-butene)	2a	305.57	436.18	2	Y	

	3a	305.35	436.16	2	Y	
	4a	305.28	436.16	2	Y	
	5a	29.36	37.44	2	Y	
	6a	26.89	38.18	2	Y	
	7a	23.29	35.89	2		
	8a	18.58	31.86	2		B from OVGF
	9a	15.97	26.32	2		B from OVGF
	10a	15.08	29.01	2		B from OVGF
	11a	14.76	27.37	2		B from OVGF
	12a	13.52	30.33	2		B from OVGF
	13a	13.04	31.07	2		B from OVGF
	14a	12.38	29.95	2		B from OVGF
	15a	11.92	32.02	2		B from OVGF
	16a	9.86	27.84	2		B from est. CCSD(T)
C_4H_8	$1a_g$	305.50	435.89	2	Y	
(trans-	$1b_u$	305.45	436.37	2	Y	
2-butene)	$2a_g$	305.33	436.15	2	Y	
	$2b_u$	305.33	436.15	2	Y	
	$3a_g$	29.29	38.61	2	Y	
	$3b_u$	26.73	35.53	2	Y	
	$4a_g$	23.90	38.10	2		
	$4b_u$	18.27	30.91	2		B from OVGF
	$5b_u$	15.06	30.49	2		B from OVGF
	$5a_g$	15.09	29.42	2		B from OVGF
	$1a_u$	14.53	24.71	2		B from OVGF
	$1b_g$	14.14	25.68	2		B from OVGF
	$6b_u$	13.27	28.92	2		B from OVGF
	$6a_g$	12.77	33.73	2		B from OVGF
	$7a_g$	11.98	32.70	2		B from OVGF
	$2a_u$	9.38	28.64	2		B from est. CCSD(T)
C_4H_8	$1a_1$	305.91	436.16	2	Y	
(isobutene)	$1b_2$	305.39	436.12	2	Y	
	$2a_1$	305.39	436.14	2	Y	
	$3a_1$	305.09	436.13	2	Y	
	$4a_1$	29.62	38.10	2	Y	
	$2b_2$	22.76	35.04	2		B from OVGF
	$5a_1$	25.21	37.71	2	Y	
	$6a_1$	17.68	34.93	2		B from OVGF
	$3b_2$	15.36	26.62	2		B from OVGF
	$7a_1$	15.22	28.96	2		B from OVGF
	$1b_1$	15.00	23.88	2		B from OVGF
	$1a_2$	13.71	26.96	2		B from OVGF

	$4b_2$	13.27	28.77	2		B from OVGF
	$8a_1$	12.90	33.96	2		B from OVGF
	$5b_2$	11.89	34.60	2		B from OVGF
	$2b_1$	9.50	27.88	2		B from est. CCSD(T)
C_6H_2	$1\sigma_g$	307.14	435.46	2	Y	
(triacet-	$1\sigma_u$	307.05	436.32	2	Y	
ylene)	$2\sigma_g$	306.85	435.66	2	Y	
	$2\sigma_u$	306.84	435.67	2	Y	
	$3\sigma_u$	306.69	436.25	2	Y	
	$3\sigma_g$	306.69	436.25	2	Y	
	$4\sigma_g$	30.43	47.40	2	Y	
	$4\sigma_u$	29.23	48.09	2	Y	
	$5\sigma_g$	27.74	49.92	2	Y	
	$5\sigma_u$	21.30	45.58	2		B from OVGF
	$6\sigma_g$	19.36	44.32	2		B from OVGF
	$6\sigma_u$	17.65	35.03	2		B from OVGF
	$7\sigma_g$	17.35	37.02	2		B from OVGF
	$1\pi_u$	12.94	27.66	4		B from OVGF
	$1\pi_g$	11.42	28.91	4		B from OVGF
	$2\pi_u$	9.55	31.73	4		B from est. CCSD(T)
C_6H_6	$1a_1$	306.22	435.99	2	Y	
(fulvene)	$2a_1$	306.07	436.11	2	Y	
	$3a_1$	305.76	435.88	2	Y	
	$1b_2$	305.74	436.11	2	Y	
	$2b_2$	305.59	436.08	2	Y	
	$4a_1$	305.59	436.09	2	Y	
	$5a_1$	31.67	38.87	2	Y	
	$6a_1$	27.97	41.44	2	Y	
	$3b_2$	26.42	42.70	2	Y	
	$7a_1$	18.21	39.00	2		B from OVGF
	$4b_2$	17.95	34.27	2		B from OVGF
	$8a_1$	17.51	33.99	2		B from OVGF
	$9a_1$	16.76	30.25	2		B from OVGF
	$5b_2$	14.99	28.67	2		B from OVGF
	$6b_2$	13.82	34.76	2		B from OVGF
	$10a_1$	13.44	41.07	2		B from OVGF
	$11a_1$	12.66	35.97	2		B from OVGF
	$1b_1$	12.57	23.77	2		B from OVGF
	$7b_2$	12.00	36.33	2		B from OVGF
	$2b_1$	9.40	27.74	2		B from OVGF
	$1a_2$	8.59	29.67	2		B from est. CCSD(T)

C_6H_6	$1a_{1g}$	305.86	435.70	2	Y	
(benzene)	$1e_{1u}$	305.84	435.86	4	Y	
	$1e_{2g}$	305.81	436.23	4	Y	
	$1b_{1u}$	305.80	436.41	2	Y	
	$2a_{1g}$	31.32	39.01	2	Y	
	$2e_{1u}$	27.64	42.09	4	Y	
	$2e_{2g}$	19.70	38.78	4		B from OVGF
	$3a_{1g}$	17.31	25.22	2		B from OVGF
	$2b_{1u}$	15.79	34.02	2		B from OVGF
	$1b_{2u}$	14.79	39.65	2		B from OVGF
	$3e_{1u}$	14.41	32.22	4		B from OVGF
	$1a_{2u}$	12.31	23.81	2		B from OVGF
	$3e_{2g}$	12.09	37.55	4		B from OVGF
	$1e_{1g}$	9.37	28.12	4		B from est. CCSD(T)
CF	1σ	718.06	1013.66	2	Y	UHF (averaged)
	2σ	309.67	436.92	2	Y	
	3σ	46.66	101.39	2	Y	
	4σ	23.40	79.50	2		B from OVGF
	1π	19.13	81.28	4		B from OVGF
	5σ	14.51	49.63	2		B from OVGF
	2π	9.45	43.27	1		B from CCSD(T)
CF_2	$1b_2$	717.93	1013.31	2	Y	
	$1a_1$	717.93	1013.32	2	Y	
	$2a_1$	312.22	436.69	2	Y	
	$3a_1$	47.66	95.30	2	Y	
	$2b_2$	45.44	106.89	2	Y	
	$4a_1$	24.30	81.58	2		B from OVGF
	$3b_2$	20.82	81.24	2		B from OVGF
	$5a_1$	19.60	75.64	2		B from OVGF
	$1b_1$	19.44	74.54	2		B from OVGF
	$1a_2$	17.31	88.09	2		B from OVGF
	$4b_2$	16.80	94.96	2		B from OVGF
	$6a_1$	12.18	56.75	2		B from CCSD(T)
CF_3	1e	717.68	1013.31	4	Y	UHF (averaged)
	$1a_1$	717.67	1013.33	2	Y	
	$2a_1$	313.60	436.43	2	Y	
	$3a_1$	47.82	92.38	2	Y	
	2e	45.39	105.15	4	Y	
	$4a_1$	24.70	82.37	2		B from OVGF
	3e	21.44	77.03	4		B from OVGF
	$5a_1$	20.07	69.93	2		B from OVGF
	4e	17.99	86.59	4		B from OVGF

	5e	17.07	90.60	4			B from OVGF
	$1a_2$	16.50	94.64	2			B from OVGF
	$6a_1$	11.02	73.10	1			B from CCSD(T)
CF_4	$1t_2$	717.96	1013.34	6	Y		
	$1a_1$	717.96	1013.36	2	Y		
	$2a_1$	316.38	436.64	2	Y		
	$3a_1$	49.21	88.29	2	Y		
	$2t_2$	45.85	104.55	6	Y		
	$4a_1$	25.49	86.13	2			B from OVGF
	$3t_2$	22.26	75.09	6			B from OVGF
	1e	18.59	83.64	4			B from OVGF
	$4t_2$	17.27	89.32	6			B from CCSD(T)
	$1t_1$	16.19	94.97	6			B from CCSD(T)
SiF	1σ	1873.43	2510.14	2	Y		UHF (averaged)
	2σ	715.46	1013.44	2	Y		
	3σ	168.38	360.56	2	Y		
	4σ	116.74	332.22	2	Y		
	1π	116.69	331.90	4	Y		
	5σ	43.23	104.29	2	Y		
	6σ	19.74	78.49	2			B partly from OVGF
	2π	16.50	80.80	4			B from OVGF
	7σ	12.52	45.02	2		3sp	B from OVGF
	3π	7.39	27.54	1		3p	B from CCSD(T)
SiF_2	$1a_1$	1874.53	2509.98	2	Y		
	$1b_2$	715.87	1013.41	2	Y		
	$2a_1$	715.87	1013.41	2	Y		
	$3a_1$	169.40	360.22	2	Y		
	$2b_2$	117.79	331.82	2	Y		
	$1b_1$	117.74	332.55	2	Y		
	$4a_1$	117.74	331.41	2	Y		
	$5a_1$	44.03	102.29	2	Y		
	$3b_2$	43.44	106.34	2	Y		
	$6a_1$	19.99	79.39	2			B from OVGF
	$4b_2$	17.98	84.31	2			B from OVGF
	$7a_1$	17.23	77.86	2			B from OVGF
	$2b_1$	16.99	77.39	2			B from OVGF
	$1a_2$	16.18	83.52	2			B from OVGF
	$5b_2$	15.80	87.63	2			B from OVGF
	$8a_1$	11.09	46.61	2		3sp	B from CCSD(T)
SiF_3	$1a_1$	1875.92	2509.91	2	Y		
	$2a_1$	716.48	1013.42	2	Y		
	1e	716.48	1013.42	4	Y		

	$3a_1$	170.67	359.78	2	Y	
	2e	119.19	331.92	4	Y	
	$4a_1$	119.15	332.32	2	Y	
	$5a_1$	44.83	101.12	2	Y	
	3e	44.11	106.11	4	Y	
	$6a_1$	21.20	80.10	2		B from OVGF
	4e	19.05	82.02	4		B from OVGF
	$7a_1$	18.19	76.02	2		B from OVGF
	5e	17.54	82.63	4		B from OVGF
	6e	16.84	85.63	4		B from OVGF
	$1a_2$	16.41	88.47	2		B from OVGF
	$8a_1$	10.61	53.01	1		B from CCSD(T)
SiF_4	$1a_1$	1876.92	2510.04	2	Y	
	$2a_1$	717.04	1013.45	2	Y	
	$1t_2$	717.04	1013.44	6	Y	
	$3a_1$	171.63	359.77	2	Y	
	$2t_2$	120.20	332.06	6	Y	
	$4a_1$	45.75	99.63	2	Y	
	$3t_2$	44.77	106.18	6	Y	
	$5a_1$	21.93	82.47	2		B from OVGF
	$4t_2$	19.73	81.00	6		B from OVGF
	1e	18.15	80.59	4		B from OVGF
	$5t_2$	17.29	84.73	6		B from CCSD(T)
	$1t_1$	16.31	88.76	6		B from CCSD(T)
OH	$1\sigma(\alpha)$	561.69	792.91	1	Y	UHF
	$2\sigma(\alpha)$	37.76	80.49	1		
	$3\sigma(\alpha)$	17.79	58.59	1		B from OVGF
	$1\pi(\alpha)$	15.97	68.94	1		B from OVGF
	$1\pi(\alpha)$	13.94	68.94	1		B from OVGF
	$1\sigma(\beta)$	560.59	795.52	1	Y	
	$2\sigma(\beta)$	33.42	71.79	1		
	$3\sigma(\beta)$	16.68	56.16	1		B from OVGF
	$1\pi(\beta)$	12.79	52.55	1		B from CCSD(T)
HO_2	1a' (α)	563.10	793.52	1	Y	
(hydro-	2a' (α)	562.63	794.31	1	Y	
peroxyl)	3a' (α)	43.02	74.60	1	Y	
	4a' (α)	28.85	85.88	1		B from OVGF
	5a' (α)	19.46	57.55	1		B from OVGF
	1a" (α)	17.30	64.42	1		B from OVGF
	6a' (α)	17.27	66.74	1		B from OVGF
	2a" (α)	12.29	77.50	1		B from OVGF
	7a' (α)	12.50	73.07	1		B from OVGF

	1a' (β)	562.43	794.62	1	Y	
	2a' (β)	561.97	795.64	1	Y	
	3a' (β)	41.29	71.78	1	Y	
	4a' (β)	27.45	80.99	1		B from OVGF
	5a' (β)	19.01	57.35	1		B from OVGF
	6a' (β)	16.70	66.31	1		B from OVGF
	1a" (β)	14.77	58.38	1		B from OVGF
	7a' (β)	11.35	71.24	1		B from CCSD(T)
CH_2O	$1a_1$	560.04	794.47	2	Y	
(formal-	$2a_1$	308.79	436.04	2	Y	
dehyde)	$3a_1$	38.38	73.38	2	Y	
	$4a_1$	21.71	44.02	2		B from OVGF
	$1b_2$	17.19	36.50	2		B from OVGF
	$5a_1$	16.24	60.83	2		B from OVGF
	$1b_1$	14.47	47.36	2		B from OVGF
	$2b_2$	10.81	54.70	2		B from CCSD(T)
CHO	1a'	561.08	794.48	2	Y	
(formyl)	2a'	308.96	436.11	2	Y	
	3a'	39.42	75.22	2	Y	
	4a'	20.61	50.28	2		B from OVGF
	5a'	17.30	53.81	2		B from OVGF
	1a"	15.39	50.69	2		B from OVGF
	6a'	14.84	53.32	2		B from OVGF
	7a'	9.20	50.07	1		B from CCSD(T)
C_2H_3O	1a'	560.12	794.56	2	Y	
(vinoxyl)	2a'	308.01	436.01	2	Y	
	3a'	306.49	435.96	2	Y	
	4a'	37.99	72.42	2	Y	
	5a'	26.12	43.16	2		B partly from OVGF
	6a'	19.80	42.09	2		B from OVGF
	7a'	16.98	40.86	2		B from OVGF
	8a'	15.78	50.53	2		B from OVGF
	9a'	14.81	34.80	2		B from OVGF
	1a"	13.74	45.58	2		B from OVGF
	10a'	10.72	57.58	2		B from OVGF
	2a"	10.20	35.04	1		B from CCSD(T)

radicals. Except for fluorine-containing radicals, we find good to excellent agreement. For H_2, the BEQ cross section in Fig. 1 is accurate enough to serve as the normalization standard for experiments. Comparisons of the BEB model to a large collection of molecules and some atoms are available from a public NIST web site: *http://physics.nist.gov/ionxsec*. The orbital constants and tables of BEB cross sections can be downloaded from the web site in the ascii format.

Encouraged by the good agreement between the BEB model and the experimental data for hydrocarbon radicals, we have included in Table 1 molecular constants for many hydrocarbons of interest to combustion modeling. Moreover, to stimulate more experimental and theoretical work and to provide data for modeling plasma processing of semiconductors with fluorine-containing molecules, we also have included in Table 1 molecular constants to generate BEB cross sections for such molecules.

ACKNOWLEDGMENTS

The present work was supported in part by the Advanced Technology Program of NIST and by the Office of Fusion Energy Sciences, the U.S. Department of Energy. We are grateful for the help we have received from Dr. W. M. Huo and Prof. M. A. Ali in generating the input data for some of the molecules presented in this article.

REFERENCES

[1] Mott, N.F., *Proc. R. Soc. London Ser. A* **126**, 259 (1930).
[2] Bethe, H., *Ann. Phys. (Leipzig)* **5**, 325 (1930).
[3] Kim, Y.-K., and Rudd, M.E., *Phys. Rev. A* **50**, 3954 (1994).
[4] Inokuti, M., *Rev. Mod. Phys.* **43**, 297 (1972).
[5] Deutsch, H., Becker, K., Matt, S., and Märk, T.D., Int. J. Mass Spectrom. **197**, 37 (2000).
[6] Gryzinski, M., *Phys. Rev.* **138**, A305 (1965); **138**, A322 (1965); **138**, A336 (1965).
[7] Rapp, D. and Englander-Golden, P., *J. Chem. Phys.* **43**, 1464 (1965).
[8] Straub, H.C., Renault, P., Lindsay, B.G., Smith, K.A., and Stebbings, R.F., *Phys. Rev. A* **54**, 2146 (1996).
[9] Nishimura, H., Huo, W.M., Ali, M.A., and Kim, Y.-K., *J. Chem. Phys.* **110**, 3811 (1999).
[10] Beran, A. and Kevan, L., *J. Phys. Chem.* **73**, 3866 (1969).
[11] Poll, H.U. and Meichsner, J., *Contrib. Plasma Phys.* **27**, 5359 (1987).
[12] Kurepa, M.V., *3rd Cz. Conf. Electronics and Vacuum Transacts.* (1965).
[13] Christophorou, L.G., and Olthoff, J.K., *J. Phys. Chem. Ref. Data* **27**, 1 (1998).
[14] Hwang, W., Kim, Y.-K., and Rudd, M.E., *J. Chem. Phys.* **104**, 2956 (1996).
[15] Huo, W.M., and Kim, Y.-K., *Chem. Phys. Lett.* **319**, 576 (2000).
[16] Kim, Y.-K., Santos, J.P., and Parente, F., submitted to *Phys. Rev. A* (2000).
[17] Basner, R., Schmidt, M., and Deutsch, H., private communication (1999).
[18] Deutsch, H., Märk, T.D., Tarnovsky, V., Becker, K., Cornelissen, C., Cespiva, L., and Bonacic-Kutecky, V., *Int. J. Mass Spectrom. Ion Processes*, **137**, 77 (1994).
[19] Peart, B., and Dolder, K.T., *J. Phys. B* **6**, 2409 (1973).
[20] Kim, Y.-K., Irikura, K.K, and Ali, M.A., *J. Res. NIST* **105**, 285 (2000).
[21] Biocchi, F.A., Wetzel, R.C., and Freund, R.S., *Phys. Rev. Lett.* **53**, 771 (1984).
[22] Tarnovsky, V., Levin, A., Deutsch, H., and Becker, K., *J. Phys. B* **29**, 139 (1996).
[23] Kim, Y.-K., Ali, M.A., and Rudd, M.E., *J. Res. NIST* **102**, 693 (1997).
[24] Becker, K., private communication (1999).

[25] Tarnovsky, V., Kurunczi, P., Rogozhinikov, D., and Becker, K., *Int. J. Mass Spectrom. Ion Processes*, **128**, 181 (1993).
[26] Becke, A.D., *J. Chem. Phys.* **98**, 5648 (1993).
[27] Lee, C., Yang, W., Parr, R.G., *Phys. Rev. B* **37**, 785 (1988).
[28] Francl, M.M., Pietro, W.J., Hehre, W.J., Binkley, J.S., Gordon, M.S., DeFrees, D.J., Pople, J.A., *J. Chem. Phys.* **77**, 3654 (1982).
[29] Purvis, G.D.I., Bartlett, R.J., *J. Chem. Phys.* **76**, 1910 (1982).
[30] Raghavachari, K., Trucks, G.W., Pople, J.A., Head-Gordon, M., *Chem. Phys. Lett.* **157**, 479 (1989).
[31] Dunning, T.H., Jr., *J. Chem. Phys.* **90**, 1007 (1989).
[32] Woon, D.E., Dunning, T.H., Jr., *J. Chem. Phys.* **98**, 1358 (1993).
[33] von Niessen, W., Schirmer, J., Cederbaum, L.S., *Comput. Phys. Rep.* **1**, 57 (1984).
[34] Zakrzewski, V.G., Ortiz, J.V., *J. Phys. Chem.* **100**, 13979 (1996).
[35] Frisch, M.J., Trucks, G.W., Schlegel, H.B., Scuseria, G.E., Robb, M.A., Cheeseman, J.R., Zakrzewski, V.G., Montgomery, J.A., Jr., Stratmann, R.E., Burant, J.C., Dapprich, S., Millam, J.M., Daniels, A.D., Kudin, K.N., Strain, M.C., Farkas, O., Tomasi, J., Barone, V., Cossi, M., Cammi, R., Mennucci, B., Pomelli, C., Adamo, C., Clifford, S., Ochterski, J., Petersson, G.A., Ayala, P.Y., Cui, Q., Morokuma, K., Malick, D.K., Rabuck, A.D., Raghavachari, K., Foresman, J.B., Cioslowski, J., Ortiz, J.V., Stefanov, B.B., Liu, G., Liashenko, A., Piskorz, P., Komaromi, I., Gomperts, R., Martin, R.L., Fox, D.J., Keith, T., Al-Laham, M.A., Peng, C.Y., Nanayakkara, A., Gonzalez, C., Challacombe, M., Gill, P.M.W., Johnson, B., Chen, W., Wong, M.W., Andres, J.L., Gonzalez, C., Head-Gordon, M., Replogle, E.S., Pople, J.A., Gaussian 98, Gaussian, Inc., Pittsburgh, PA, 1998.
[36] Schmidt, M.W., Baldridge, K.K., Boatz, J.A., Elbert, S.T., Gordon, M.S., Jensen, J.H., Koseki, S., Matsunaga, N., Nguyen, K.A., Su, S.J., Windus, T.L., Dupuis, M., Montgomery, J.A., *J. Comput. Chem.* **14**, 1347 (1993).